Available online at http://www.journalcra.com

International Journal of Current Research
Vol. 9, Issue, 10, pp.59757-59761, October, 2017

INTERNATIONAL JOURNAL OF CURRENT RESEARCH

ISSN: 0975-833X

RESEARCH ARTICLE

SPECTROSCOPIC AND DIAGNOSTIC ANALYSIS OFA HIGH POWER AC PLASMATRON

***,[1]Özge Yazıcıoğlu, [1]T. Yaşar Katırcıoğlu and [2]ÜmmügülErözbek Güngör**

[1]AR&TeCS AnadoluAr-Ge Teknoloji Mühendislikve Danışmanlık A.Ş., Ankara, Turkey
[2]Department of Physics, Middle East Technical University, 06800 Ankara, Turkey

ARTICLE INFO

Article History:
Received 29th July, 2017
Received in revised form
24th August, 2017
Accepted 13th September, 2017
Published online 31st October, 2017

Key words:
Plasmatron, Arc Jet,
Atmospheric plasma,
OES, Plasma diagnostic.

ABSTRACT

This paper presents the experimental characterization of an atmospheric (atm) pressure, high-power alternating-current (AC) three-phase plasmatron established in AR&TeCS Inc. by using optical emission spectroscopy (OES) method. Power of the arc plasma jet changes in the range of 590-1100 kW. At each power, emission of the jet is collected by an fiber optic spectrometer (200-1100 nm). The atm plasma is mainly dominated by the nitrogen species in the visible range. The strongest nitrogen atomic line (NII or N^+-singly ionized) is detected at 510.45 nm. The others are observed at 589.32, 606.50 and 617.33 nm. The electron temperature (T_e) is replaced by the excitation temperature (T_{ext}) according to the assumption of local thermodynamic equilibrium (LTE). The calculated T_e is in the range of 11654-12400 K. The electron density (n_e) is determined from the equation that is referred by McWhirter. The value of the density changes around 10^{-21} m^{-3}. The both T_e and n_e increase with the arc power up to 950 kW and then a sharp decrease is clearly observed. After 1 MW power, the decrease becomes stable.

Citation: Özge Yazıcıoğlu, T. Yaşar Katırcıoğlu and ÜmmügülErözbek Güngör, 2017. "Spectroscopic and diagnostic analysis of a high power AC plasmatron", *International Journal of Current Research*, 9, (10), 59757-59761.

INTRODUCTION

Plasma technology has been developed in different concepts of plasma–non-thermal, thermal, low pressure or atmospheric pressure. Plasmatron is a device that converts the electrical energy to the thermal energy based on heat conductivity and convective heat exchange between the arc and the gas flow (Zhukov and Zasypkin, 2007). Plasmatrons are used in many high temperature technologies such as gasification and combustion of biomass, coal and all type of wastes, simulating the re-entry conditions of aircrafts into atmosphere, testing of heat protection materials and scientific research (Yazicioglu and Katircioglu, 2017). Electron temperature (T_e) and electron number density (n_e) are two important parameters to describe the physical structure of the plasma. These parameters are mostly monitored by the techniques such as Langmuir probe, interferometry, mass spectroscopy and optical emission spectrometry (Devia *et al*., 2015). Among these techniques, OES is the simplest and unperturbative method that is used to determine the specifications of plasma at wide temperature and pressure ranges. Different methods have been developed for different plasma types to analyze plasma via OES. In atmospheric thermal plasmas, collisions increase with high pressure. By this way, the electrons transfer their energyto the other heavy particles.

***Corresponding author:* Özge Yazıcıoğlu,**
AR&TeCS AnadoluAr-Ge Teknoloji Mühendislikve Danışmanlık

Then, the electron temperature approaches gas temperature. Therefore, local thermodynamic equilibrium conditions are generally valid in atmospheric thermal plasmas. In the OES method, the emitted light, which are coming from the plasma, are collected by a fiber optic spectrometer. These electromagnetic (EM) radiations are represented in an intensity-wave length graph. Particles (atoms, molecules and ions) that collide with the free electrons in the plasma gain energy and then the bounded electrons inside these particles are excited to rise from low energy level to high energy level. Since the excited electrons are not stable, they emit energy as photons as they go back to low energy level. The emitted photon energy is equal to the difference in the low and high energy levels (Fantz, 2006). The wavelength of the emitted photon is expressed by the difference between the excited (E_2) and ground (E_1) energy levels of the electrons as given in the following equation;

$$\lambda = \frac{hc}{E_2 - E_1} \quad (1)$$

There are different plasma models such as the local thermal equilibrium, the steady-state corona model, the time-dependent corona model and the collisional radiative model to estimate plasma properties. Among these models, the most suitable one is preferred according to the structure of the plasma (Garamoon *et al*., 2007). These different methods are introduced in the following sections.

Local Thermal Equilibrium

In this model, the electron density is sufficiently high and the collisions with the electrons are dominant in the radiative processes (Numano *et al*., 1990). Boltzmann and Saha equations govern the population distribution of LTE plasmas and the electron energy distribution function (EEDF) is assumed to be Maxwellian. The radiation field in LTE plasmas depends on local plasma conditions, population distributions and atomic transition probabilities (Ley *et al*.,). For the LTE assumption, McWhirter proposed a criterion given as the following equation (McWhirter, 1965);

$$n_e \geq 1.6x10^{12}(T)^{1/2}(\Delta E)^3 \quad (2)$$

Where $n_e(cm^{-3})$ is the electron density, T (K) is the plasma temperature and ΔE(eV) is the energy gap. In the results section, the minimum value of the electron density is determined by means of the Equation (2).

Maxwellian Distribution Theory

A group of particles throughout a plasma space under no external disturbance tend to reach thermal equilibrium due to particle collisions. To describe such distribution of particles Maxwellian Distribution Theory is used. The distribution of the particles that compose the plasma is introduced with respect to their velocities in this theory. The density, *dN*, of any particles with velocities in the *v+dv* range can be described as *dN=Nf(v)dv*, where N is the density of the particles and *f(v)* is the Maxwell velocities distribution function (Devia *et al*., 2015):

$$f(v) = 4\pi r^2 \left(\frac{m}{2\pi kT}\right)^{3/2} exp\left(-\frac{mv^2}{2kT}\right) \quad (3)$$

Where *k* is Boltzmann's constant (1.3810^{-23}J/K), *m* is the mass of the particle and *T* is the temperature. In our system, the atm arc plasma shows a Maxwellian distribution (Haar, 1995).

Coronal Model

A coronal model can describe plasma state when the electron density is low (~10^{12} m^{-3}) and the electron temperature is high (~100 eV) which is often seen in astrophysical situations, such as in the corona region in the Sun. In such plasmas, because of the fact that the electron density and the radiation field are so low, collisional de-excitations and three body recombinations are insignificant and can be neglected. On the other hand, the electron temperature in the coronal model plasma is very high. Each particle species (electrons, ions and neutrals) is characterized by its own temperature ($T_e > T_i \geq T_n$). The corona plasma is characterized by a low degree of ionization (Fantz, 2006). Condition for corona model that has limited range of the electron density can be expressed as (McWhirter, 1965);

$$n_e \leq 5.6x10^8(z+1)[T_e]^{1/2} exp\left[\frac{1.162x10^3(z+1)^2}{T_e}\right] \quad (4)$$

where z is an ionic charge, $n_e(cm^{-3})$is the electron density and T_e(eV) is the electron temperature.

Collisional Radiative Model

In a collisional-radiative (CR) model, collisional and radiative processes are balanced (Fantz, 2006).Unlike LTE model, the population distribution at any point in the plasma region does not depend only on the plasma parameters at that point. Also, as distinct from the coronal plasmamodel, the population distributions are affected by the collisional depopulation processes and stepwise collisional processes in the CR plasma model. Laboratory plasmas in different regimes of the electron density and the temperature can be observed frequently in CR plasma model (Chung, *et al*., 2008).

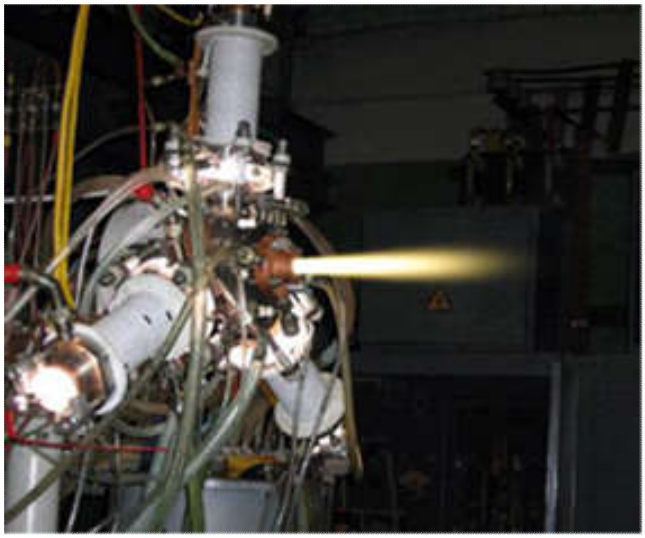

Figure 1a. Photograph of a 1MW AC plasmatron

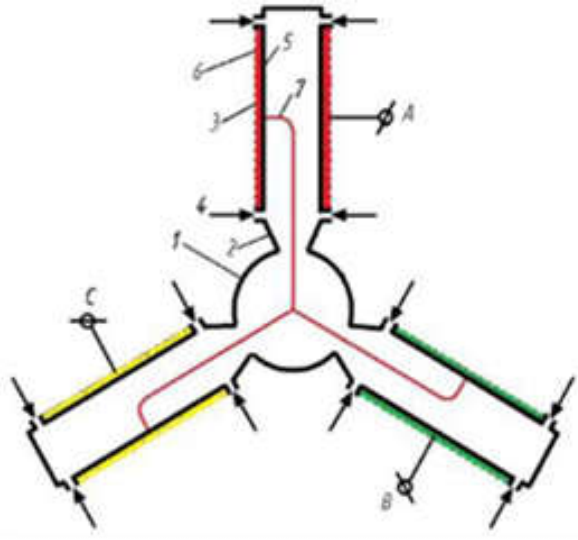

Figure 1b. Design of the plasmatron

Condition for CR model can be expressed in the following equation (Griem, 1964);

$$n_D = 2.6x10^5 \left[\frac{(z+1)^2 T_e}{(1+Z_{eff})n_e}\right]^{1/4} \quad (5)$$

Where n_D is th ehydrogenic principal quantum number, $n_e(cm^{-3})$ is the electron density, T_e(eV) is the electron temperature, z is theionic charge and Z_{eff} is the charge state of plasma.

Experimental set-up

In this paper, plasma parameters (the electron temperature and the electron density) of a high power AC three-phase plasmatron in AR&TeCS Facility were experimentally studied with using OES method. Also, the effects of different arc

powers on the plasma characteristics are investigated. The home-made plasmatron shown in Figure 1 (a) has been designed at Keldysh Research Center. The schematic diagram of the plasmatron is clearly seen in Figure 1 (b). The set-up of the plasmatron is basically composed of three identical arc chambers that are merged by a mixing chamber (1). The each arc chamber has a constrictor (2), an electrode (3) and two insulators (4). Copper cylindrical electrode (5) and magnetic coil (for an arc root rotation) (6) are placed on the electrode unit and there is a water jacket for the electrode cooling (not shown in the Figure 1 (b)). All the electrode units are connected to the each other with one-phase of supplying three-phase electric lines (7). Therefore, the each arc is generated between the electrode and the plasma and they are mixed at the center (star point) of the circular chamber (Svirchuk and Golikov, 2016).The plasmatron test system established at AR&TeCS consists of five main sub-systems including electrical system, cooling system, air supplying system, ventilation system, data acquisition (DAQ) and control system. First of all, the cooling and the air supplying systems turn on. Then, the power is supplied and the discharge current is constituted between the electrodes and the constrictors. This current generates the arc plasma as soon as interacting with the feed gas. The arc that starts to rotate by interacting with the magnetic field accelerates in the constrictor and merges at the star point and then it goes out of the nozzle at the exit of the mixing chamber. Emission spectrums of the arc plasma are collected by an Ocean Optics HR-4000-UV-NIR model spectrometer, which can measure the plasma flow at the exit of the plasma nozzle at 200-1100 nm wavelength. Figure 2 shows the general schematic of our experimental set-up in which data is acquired with the optical spectrometer. The spectrometer is positioned 53.5 cm away from the plasma flow and receiving data from the first 5.5 cm of the flow.

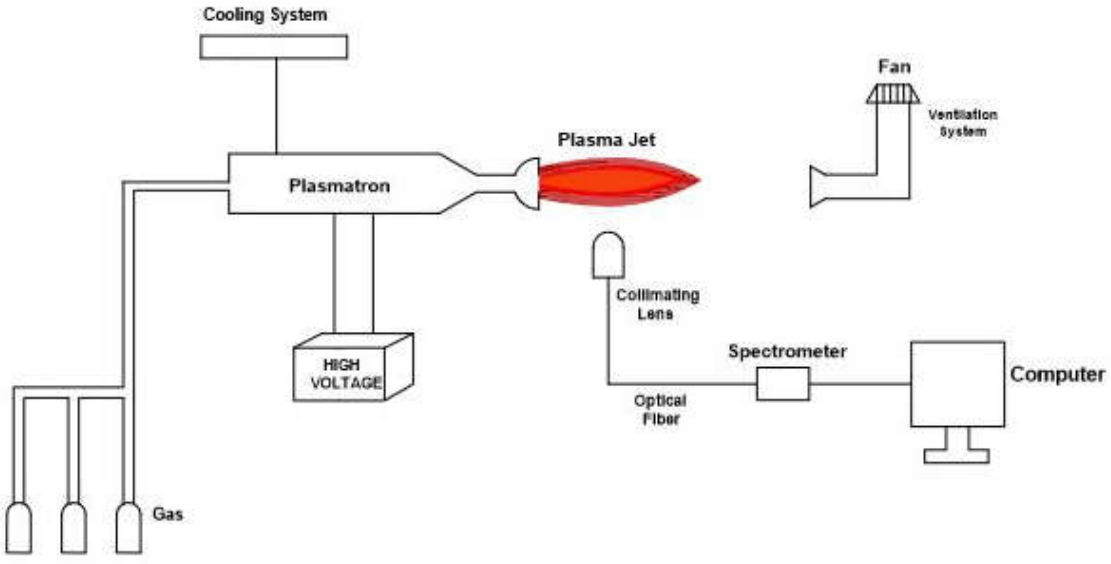

Figure 2. Schematic diagram of the Plasmatron Test System in AR&TeCS Facility

RESULTS AND DISCUSSION

Since the plasmatron works at atmospheric pressure, high pressure increases collisions between the electrons and the heavy particles and so the electron temperature approaches to the gas temperature. By this way, local thermodynamic equilibrium (LTE) model is applicable for this type of plasma (Garamoon *et al*., 2007, Laux *et al*., 2003 and Andreas *et al*., 1998). The electron temperature and the electron density are determined according to the LTE model and the profiles of these parameters with respect to the arc power are mentioned. In our atm arc plasma, many atomic and molecular lines of Nitrogen (N) and Oxygen (O) are detected in the OES spectrums. The most dominant (78%) gas in the air is Nitrogen. Therefore, plasma parametrical calculations were done according to the emission atomic lines (NI-neutral and NII-singly ionized) of this gas. A detailed sample OES spectrum of the plasma is clearly observed in Figure 3. An increase in the population of the particles directly increases the intensity of spectral lines (Kolpakova *et al*., 2011). As seen from the Figure 3, the most dominant peak in the visible range belongs to the NII atom at 510.45 nm. This atomic line originates from the transition of inner-shell excited electronic configuration $2s^22p3p\,^1S$ - $2s^22p4s\,^1P°$. The other NII lines are observed at 589.32 nm with the transition of $2s2p^2\,(^4P)3s\,^3P$ - $2s2p^2(^4P)3p\,^3D°$, at 606.50nm with the transition of$2s^22p3p\,^3P$ - $2s^22p3d\,^1D°$ and at 617.33 nm with the transition states of $2s^22p3d\,^3F°$ - $2s^22p4p\,^3D$(NIST, 2017).The relation between the intensity and the arc power at different wavelengths is investigated as shown in Figure 4. From the Figure 4, the peak at 510.45 nm is mostly affected by the change of arc power. A sharp intensity decrease up to almost 850 kW is observed and then it increases almost linearly. The other peaks show very similar variation with the arc power especially at 606.50 and 617.33 nm. Up to almost 850 kW, the intensities of these peaks increase with the power slowly and then abruptly. The key point is that all the variations become stable at 1000 kW that is the optimum level for the arc power.

Determination of Electron Temperature and Electron Density: In plasma environment, particles (atoms, molecules and ions) hit to the free electrons and gain energy. The bounded electrons of these particles jump from low energy level to high energy level. Photons are emitted when the electrons pass back to low energy level. The energy difference between the low and high energy levels is E_2-E_1=hc/λas given in the Equation 1 where λ is the wavelength of the emitted photon, h is the Planck constant and c is the velocity of light. In the local thermodynamic equilibrium method, the electron temperature is calculated according to the following formula (Zhi *et al*., 2007).

$$ln\left[\frac{I_2\lambda_2}{g_2A_2}\right] = -\frac{1}{kT}E_2 + b \quad (6)$$

In this equation, I_2 is the high level intensity of light, $\lambda_2$is the high level wavelength, $g_2$is the statistical weight, $A_2$is the Einstein transition probability and E_2 is the high energy level, k is the Boltzmann constant, T is the excitation temperature, and b is the constant. Two parameters, $\lambda_2$and I_2, are obtained from the I-λOES spectrum and the values of g_2, A_2 and E_2 are obtained from the National Institute of Standards and Technology (NIST, 2017). The electron temperature can be determined by the Boltzmann plot. A plot of $ln\left[\frac{I_2\lambda_2}{g_2A_2}\right]$ versus E_2 gives a straight line with a slope of $-1/kT$ .The spectral emission lines of NII are listed in Table 1 for Boltzmann plot to determine the plasma electron temperature.

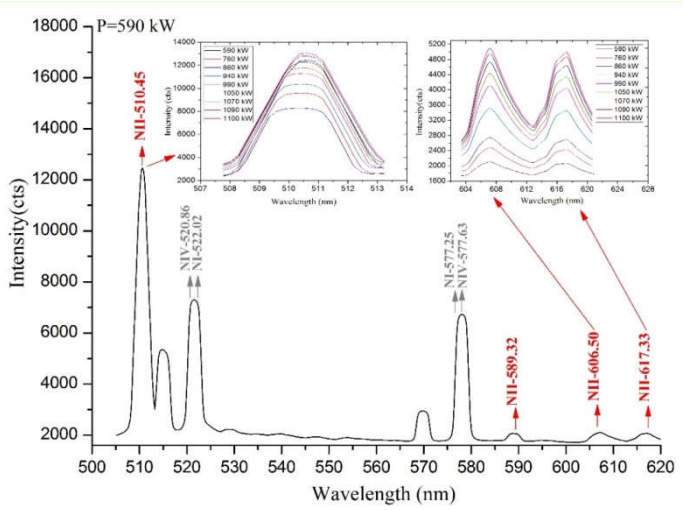

Figure 3. The emission spectrum of arc plasma at 590 kW with the power evolutions of specified NII peaks

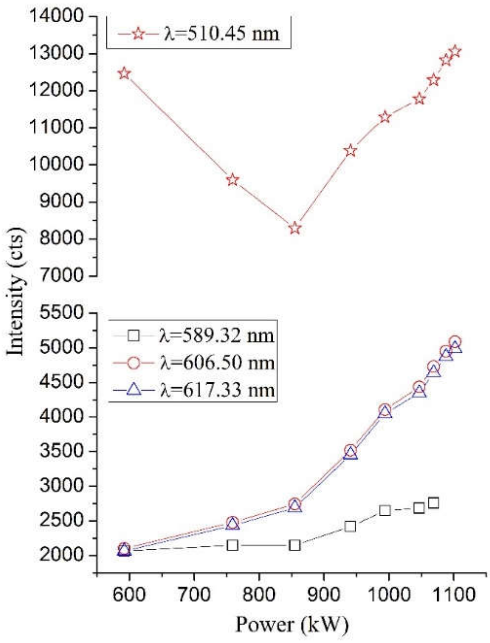

Figure 4. The evolution of the intensity of NII peaks with respect to the arc plasma power

For the power 590 kW, the Boltzmann plot is given as in Figure 4, the electron temperature is calculated as 11654 K (~1eV). The best fit is drawn according to the most intense peak at 510.45 nm. The results show that the range of the electron temperature changes from 11654 K to 12400 K as the power changes from 590 kW to 1100 kW.

Table 1. Spectral atomic line parameters of singly ionized nitrogen-NII

Wavelength (nm)	g_2	A (s^{-1})	E_2 (cm^{-1})	Intensity (cts)
510.45	3	1.01E+07	197858.69	12460.82
589.32	7	2.88E+07	228791.80	2063.27
606.50	5	2.57E+05	187091.40	2100.32
617.33	5	2.62E+07	202861.40	2063.00

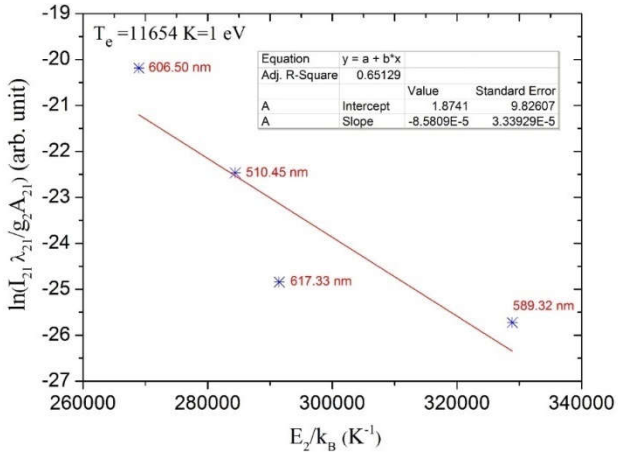

Figure 5. Linear Boltzmann plot of the NIIpeaks to estimate the electron temperature

The minimum value of the electron density is determined according to the McWhirter criterion as given in the Equation 2. In this equation, the plasma temperature is replaced by the excitation temperature (T_i=T_e=T_{exc}). For the neutral Nitrogen atoms (NI), ΔE is 2.15 eV. The range of the electron densities is between $1.69x10^{-21}$ $m^{-3}$and $1.72x10^{-21}$ m^{-3} in accordance with the literature suggested that $n_e \geq 10^{20}m^{-3}$ for the arc plasmas and the plasma torches (Castillo and Blanco, 2016).In study of an example of plasma jet in atmospheric pressure, the electron temperature and the electron density are estimated about 0.61 eV and $4.38x10^{21}$ m^{-3}, respectively (Aadim *et al*., 2015). In another study of an atmospheric pressure plasma jet, the electron temperature is about 1.0 eV and the electron density is $4.3x10^{22}$ m^{-3}, which was determined under the assumption of LTE (Förster *et al*., 2005). Also, atmospheric pressure air plasma in LTE, the electron temperature is calculated as 1 eV (11600 K) and the electron density is estimated about $1.0x10^{21}$ m^{-3}(Laux *et al*., 2003).

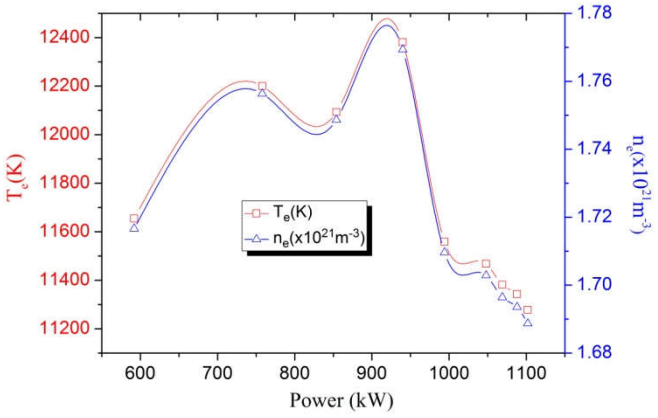

Figure 6. The evolutions of T_e and n_e with respect to the arc plasma power

The power dependence of the electron temperature and the electron density are given in Figure 6. The both parameters increase to a power 950 kW and then start to decrease. From the 1000kW (optimum power) to 1100 kW, a steady decrease is observed. The results show that the electron temperature and the electron density have significant dependence on the power. The reason of this is that the energy is first transmitted to the free electrons and then transferred to the other heavy particles (ions and neutrals) as a result of the collisions. Because of its low mass, the electrons are more active than the other particles and their temperatures are higher than the temperatures of other particles. However, as the number of collisions increase, the temperatures of other particles increase (Moisan and Pelletier, 2012). With the increasing power, first free electrons gain more energy and so the electron density and the electron temperature increase up to a certain value at 950 kW. Plasma starts to be stabilized at the power about 1000 kW. As the electrons transfer their energy to the other particles, the electron temperature decreases. Also, the ionization rate increases at these levels, so the electron density decreases while the ion density increases.

Conclusion

High power atmospheric pressure AC plasmatron was investigated by optical emission spectrometry technique by non-intrusively. The LTE model that is applicable for the atmospheric thermal plasmas is used to estimate the plasma parameters (Yazicioglu *et al*., 2017). Calculation was based on singly ionized nitrogen ions, NII. When the intensity-wavelength spectrum is analyzed, the most intense peak is observed at 510.45 nm and the others are at 589.32, 606.50 and 617.33 nm. By analyzing the intensity-power relation, the peak of 510.45 nm shows a different characteristic with the power as decreasing to 850 kW, and then it starts to increase. At the power 1000 kW, which is the optimum working value for plasmatron, the intensities increase steadily with the power. The electron temperature is determined by the means of Boltzmann plot and the LTE condition. The temperature changes from 11654 K to 12400 K. The McWhirter criterion was used to measure the electron density and it is shown that the density is between $1.69x10^{-21}$ m^{-3} and $1.72x10^{-21}$ m^{-3}. The electron temperature and the density values increase to a power 950 kW and then it starts to decrease. From the 1000 kW (optimum power) to 1100 kW, a steady decrease is observed. The electrons transfer their energy to other heavy particles and so the electron temperature decreases at 1000 kW (optimum power) in which plasma starts to be stabilized. Also, the ionization rate increases at the optimum level, the electron density decreases. In future work, the electron density and the electron temperature will be analyzed according to distance.

REFERENCES

Aadim, K. A., Hussain, A. A-K., Abdalameer, N. K., Tawfeeq H. A., Murbat, H. H. 2015. *International Journal of Novel Research in Physics Chemistry & Mathematics* Vol. 2, Issue 2, pp: (28-32).

Asenjo-Castillo, J., Vargas-Blanco, I. 2016. Emissions pectroscopy of an at mospheric pressure plasma, Espectroscopia de Plasmas en condiciones de presiónatmosférica, Vol. 29, Número Especia lEstudiantes 3. Pág 47-58. DOI: 10.18845/tm.v29i6.2901.

Chung, H. K., Lee, R. W., Chen, M. H., Ralchenko, Y. 2008. The How To For Flychk @NIST.

Devia D. M., Rodriguez-Restrepo, L. V., Restrepo-Perra, E. 2015. Methods Employed in Optical Emission Spectroscopy Analysis: a Review, PACS: 52.25.Dg, 31.15.V-doi:10.17230/ingciencia.11.21.12.

Fantz, U. 2006. Basics of plasmaspectroscopy, Plasma SourcesSci. Technol. 15; S137-S147, doi:10.1088/0963-0252/15/4/S01.

Förster, S., Mohr, C., Viöl, W., 2005.Investigations of an at mospheric pressure plasma jet by optical emissions pectros copy, Elsevier, Surface & Coatings Technology, 200, 827-830.

Garamoon, A. A., Samir, A., Elakshar, F. F., NosairA. And Kotp E. F. 2007. SpectroscopicStudy of Argon DC Glow Discharge, IEEE Transactions on Plasma Science, vol. 35, no.1.

Griem, H. R. 1964. Plasma Spectroscopy, McGraw-Hill.

Haar, D. 1995. Elements of Statistical Mechanics. Elsevier Science.

Kolpakova, A., Kudrna, P., Tichy, M. 2011. Study of Plasma Systemby OES (Optical Emission Spectroscopy), WDS'11 Proceedings of Contributed Papers, Part II, 180-185, ISBN 978-80-7378-185-9.

Laux,C. O., Spence, T. G., Kruger C. H. and Zare, R. N., 2003. Optical diagnostics of at mospheric pressure air plasmas, Plasma Sources Sci. Technol. 12, 125-138.

Ley, H. H., Yahaya, A., Ibrahim, R. K. R. Analytical Methods in Plasma Diagnosticby Optical Emission Spectroscopy: A Tutorial Review Department of Physics, Universiti Teknologi Malaysia, 81310 Skudai Johor.

McWhirter, R. W. P. 1965. Spectralintensities, Plasma Diagnostic Techniques, New York, Academic Press. p. 206.

Moisan, M., Pelletier, J. 2012. Physics of Collisional Plasmas: Introduction to High-Frequency Discharges, ISBN 978-94-007-4558-2.

NIST, National Institute of Standards and Technology, 2017. https://www.nist.gov/pml/atomic-spectra-

Numano, M. 1990. Criteria For Local Thermodynamic Equilibrium Distributions of Populations of Populations of ExcitedAtoms in a Plasma, *J. Quant. Spectrosc. Radit. Transfer* Vol. 43, No.4, pp. 311-317.

Schutze, A., Jeong, J. Y., Babayan, S. E., Park, J., Selwyn, G. S. and Hicks, R. F. 1998. The Atmospheric-Pressure Plasma Jet: A Review and Comparison to Other Plasma Sources, IEEE Transactions on Plasma Science, vol. 26, no.6.

Svirchuk, Y. S., Golikov, A. N. 2016. Three-Phase Zvezda-Type Plasmatrons, IEEE Transactions on Plasma Science, Vol. 44, No.12.

Yazicioglu O., Katircioglu T.Y., İbrahimoglu, B. 2017. Temperature Measurement of High Power Plasmatron Plasma Flow Using Optical Emission Spectroscopy, Sares, Sustainable Aviation Research Society, Sühad, in Turkish, 10.23890/suhad.2017.0102.

Yazicioglu, O., Katircioglu, T. Y. 2017. Applications of Plasma Technology in Energy Sector, Kırklareli UniversityJournal of EngineeringandScience, 3, 1 18-44.

Zhi, S.X., Ping, Y., Ming, Z.H., Jie, W. 2007. Transition probabilities for NII 2p4f–2p3d and 2s2p23d–2s2p23p obtained by a semiclassical Method", IOPscience, no:10, 2934-2936.

Zhukov M.F. and Zasypkin I.M., 2007. Thermal Plasma Torches Design, Characteristics, Applications, ISBN 978-1-904602-02-6.

****